

Effects of particle shape irregularity on the microstructure of granular materials

Duc-Cuong Pham^{1,2}, Duc-Hanh Nguyen², Lhassan Armasid³, and Farhang Radjai^{1,*}

¹LMGC, University of Montpellier, CNRS, 163 rue Auguste Broussonnet, 34090 Montpellier, France

²Inhytech, HEC, Hanoi University of Civil Engineering, 55 Giai Phong street, Hanoi, Vietnam

³CEA, DES, IRESNE, DEC, Cadarache, F 13108 Saint Paul lez Durance, France

Abstract. We use 3D simulations by discrete element method to explore the effects of particle-to-particle shape irregularity on the microstructure and force transmission in granular packings. Using modified icosahedra with a controlled degree of irregularity, we prepare large frictionless samples by isotropic compaction. We show that local order decreases with increasing shape irregularity, as evidenced by a flattened first peak in the radial distribution function while the mean inter-particle distance for nearest neighbors remains stable. Furthermore, while the samples are isostatic, the contact network topology varies with shape irregularity: the proportion of stabilizing face-face contacts decreases while weaker single contacts become more prevalent. This structural change leads to an increase in force network inhomogeneity, evidenced by a broader probability distribution of normal contact forces with a larger population carrying weak forces. These combined microstructural changes suggest potential consequences for the macroscopic mechanical response under shear, such as a possible decline in the internal friction coefficient. This work underscores the critical role of statistical shape variability in controlling granular fabric and force transmission, offering insights for modeling natural and engineered granular materials.

1 Introduction

The mechanical behavior of granular materials is strongly influenced by particle shape. While discrete element method (DEM) simulations increasingly account for complex particle geometries, most systematic studies focus primarily on the effects of average shape characteristics, such as angularity or elongation [1–6]. However, the impact of shape variability around these mean values is rarely, if ever, addressed.

The statistical shape “noise” or variability is inherent in natural and industrial particles such as crushed rock and cohesive fine powders. It can significantly alter packing structure and force transmission as illustrated by extensive 2D DEM simulations by Nguyen et al. [7]. A systematic approach for the quantification of the effects of shape variability consists in applying controlled perturbations to a reference shape. For example, in Ref. [8], pentagons were used as reference shape and they were made irregular by randomly moving the vertices within an angular range. The authors showed that, at low size polydispersity, the range of shape variability profoundly affects the microstructure, and the shear strength (internal friction angle) declines with increasing irregularity. This framework opens avenues to show how and which specified aspects of shape noise drive changes in granular behavior, thereby moving towards a more fundamental understanding than comparisons of disparate natural shapes can typically provide.

In this work, we apply this perturbative approach to investigate the effects of shape irregularity in 3D by considering regular icosahedron as reference shape. Particles are made irregular by introducing controlled, random perturbations to their vertices within a prescribed maximum displacement. This technique allows us to create a continuous spectrum of particle shapes where the degree of irregularity is systematically tuned via a single parameter representing the normalized vertex displacement magnitude. We consider isostatic packings generated by isotropic compaction of these particles with fully periodic boundary conditions. We present the effects of the systematically varied shape irregularity on key microstructural properties including packing density, local order, contact network, and force distributions.

2 Numerical Model

We modeled particles as irregular polyhedra generated by perturbing the vertices \mathbf{v}_i^0 of a regular icosahedron of edge length L . Each vertex was randomly displaced within a spherical sector $\mathbf{v}_i = \mathbf{v}_i^0 + r\mathbf{u}(\theta, \phi)$ centered on the vertex, where \mathbf{u} is a random unit vector in spherical coordinates $\theta \in [0, \delta]$, $\phi \in [0, 2\pi]$. The ratio r/L defines the degree of shape randomness. Seven samples of 8000 particles of unique shapes, corresponding to different values of r/L , were prepared using 3D DEM simulations employing fully periodic boundary conditions to remove wall effects. We used the in-house Rockable

*Corresponding author: farhang.radjai@umontpellier.fr

code designed for the simulation of arbitrary particle shapes based on spheropolyhedral elements [9] with implemented Minkowski radius R_m to smooth the sharp edges and vertices of particles. In this approach, the vertices and edges are replaced by spheres and cylinders of radius R_m . This mathematical approach makes contact detection and force calculation more efficient while maintaining accuracy. In our simulations we fixed $R_m = 0.1L$.

Note that each sample is characterized by a given value of r/L , but within the sample the positions of the vertices of each particle are uniformly distributed in the range $[0, r]$. In other words, up to a maximum value r , each particle has a unique shape. Simulations were performed with frictionless particles ($\mu_s = 0$) in order to obtain uniquely defined random close packings. With three-periodic boundary conditions, the isotropic compaction occurs under the action of a constant average compressive pressure σ_0 . Initially, the particles are randomly placed inside the simulation cell. The pressure σ_0 acts on the six collective degrees of freedom, which replace the wall degrees of freedom. As these collective degrees of freedom move, they induce affine displacements of the particles. The compaction dynamics is therefore a consequence of the joint effects of the induced affine displacements and the nonaffine motions arising from contact interactions between particles. This process is allowed to continue until a stable equilibrium state is achieved. In this final state, the kinetic energy is negligible as compared to the overall elastic energy and the contact network remains stable. Furthermore, the internal pressure is equal to the imposed pressure σ_0 .

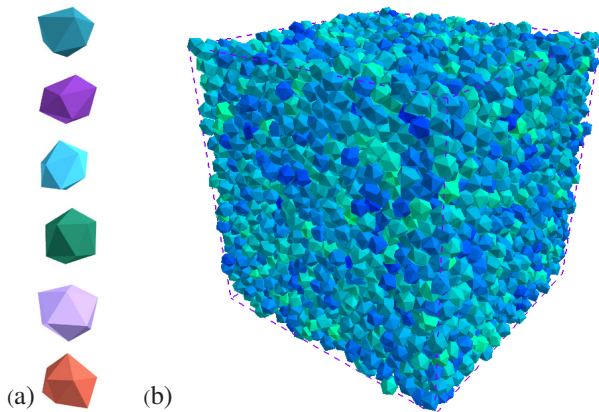


Figure 1. (a) Examples of the irregular icosahedral particles with irregularity $r/L = 0.15$. (b) A sample of 8000 irregular icosahedra with $r/L = 0.15$. Dashed lines indicate cell boundaries and color intensity is proportional to particle volume.

3 Packing fraction

Figures 1(a) and 1(b) show snapshots of particles and a typical jammed packing. Fig. 2 displays the packing fraction Φ in the isostatic state as a function of r/L . Its value is stable around ≈ 0.68 for $r/L \leq 0.075$ before increasing to ≈ 0.69 at $r/L = 0.15$. This suggests

that minor surface perturbations might be accommodated locally within the packing structure without significantly altering the overall space-filling efficiency.

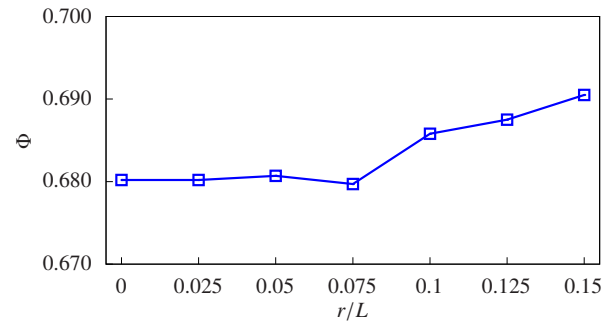


Figure 2. Packing fraction Φ as a function of the irregularity parameter r/L .

By introducing sufficient statistical irregularity, the symmetry breaks down and leads to shape polydispersity and a small size polydispersity that enables particles to explore a broader range of configurations, leading to a more locally disordered but higher global density state. The effect of shape irregularity depends also on the reference shape. Icosahedral particles are close to sphere so that the applied transformations do not represent an appreciable perturbation of the shape as compared to spheres. Below, we will see that they do have an effect on other microstructural properties of the packings.

4 Pair distribution function

Local structure was analyzed using the radial distribution function (RDF) $g(R) = n(R)/n$, where $n(R)$ is the number density at distance R from a particle and n is the bulk density [8]. We normalize R by the mean particle diameter $\langle d \rangle$. The particle diameters d are defined via equivalent particle volume between each particle and a sphere of diameter d . As shown in Figs. 3, increasing r/L drastically reduces the height and increases the width of the first peak of $g(R)$, which is located near $R \approx 0.97\langle d \rangle$, while the valley between the first and second peaks becomes shallower. This indicates that statistical shape irregularity significantly disrupts the local positional ordering of particles, even though the average nearest-neighbor distance is stable.

The shoulder observed near $R/\langle d \rangle \approx 0.94$ in the RDF for regular icosahedra ($r/L = 0$) is explained by the dominance of edge-edge contacts (78% of total contacts). This specific distance corresponds to a preferred configuration related to twice of center-to-edge distance of icosahedra $r_e/\langle d \rangle \approx 0.445$. Irregularity disrupts this precise configuration, broadening the distance distribution and causing the shoulder to be less pronounced.

5 Contact network

We analyzed the contact network topology by classifying contacts based on vertex/edge/face interactions. Face-face contacts represent three independent geometrical

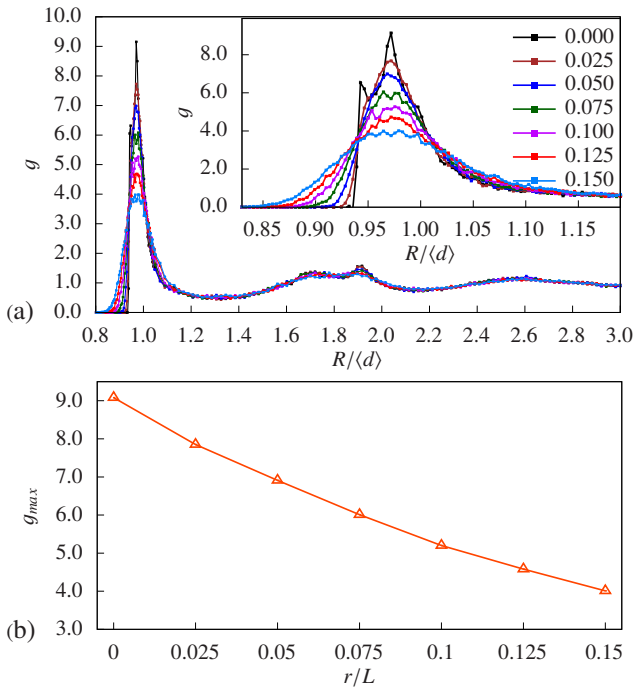


Figure 3. (a) Radial distribution function $g(R)$ for different r/L values. Inset is a zoom on the first-neighbor peak. (b) First peak amplitude g_{max} as a function of r/L .

constraints. For this reason, they are denoted as “triple” contacts. In the same way, edge-face contacts are “double” contacts in the sense that they are characterized by two independent constraints. All other contacts are “simple” contacts. In the simulations, the face-face and edge-face contacts are treated by attributing several points of contact to each contact. The total interaction force at such contacts is the sum of the calculated forces at the point contacts. We therefore distinguish the three types of contacts and their corresponding proportions N_s (simple), N_d (double), and N_t (triple), respectively [8, 10].

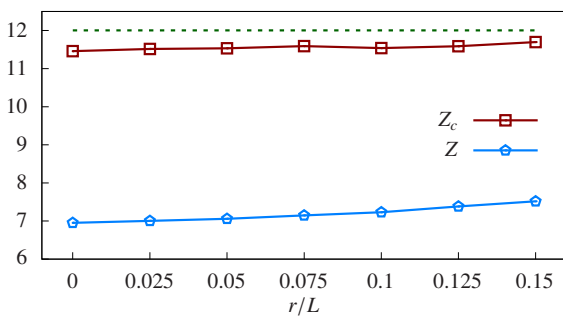


Figure 4. Coordination number Z and constraint number Z_c as a function of shape irregularity r/L .

Accordingly, we distinguish between the usual coordination number Z as the average number of contact neighbors of a particle and the *constraint number* Z_c defined as the number of independent constraints [10]:

$$Z_c = \frac{2(N_s + 2N_d + 3N_t)}{N_p}$$

where N_p is the total number of particles. Fig. 4 shows the evolution of Z and Z_c with r/L . Z_c remains constant at $Z_c \approx 12$ while Z slightly increases with r/L indicating the frictionless packings are isostatic regardless of irregularity. To obtain the values of Z_c , we assume that the packings are isostatic due to zero friction. In our packings, each particle has $N_f = 6$ degrees of freedom (3 translations and 3 rotations), and the average number of normal forces per particle is $Z_c/2$ since each contact is shared by two particles. The condition of isostaticity implies $N_f = Z_c/2$, leading to $Z_c = 6$ for spheres and $Z_c = 12$ for isosahedra.

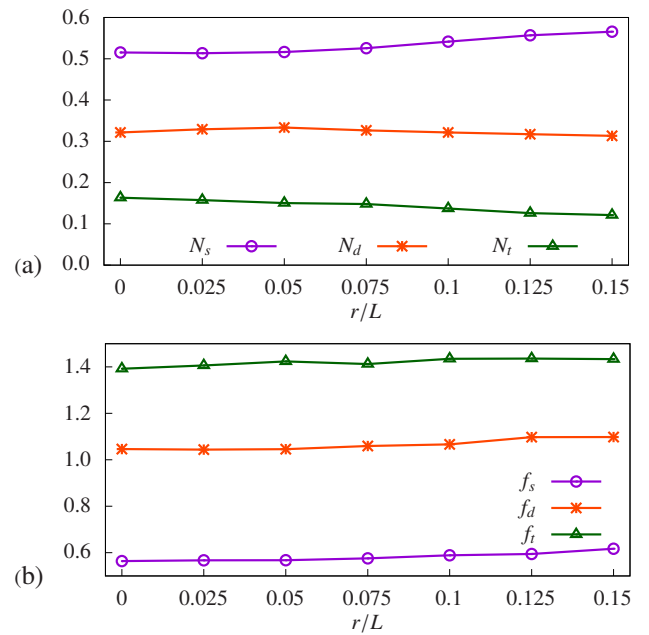


Figure 5. (a) Proportions of triple (N_t), double (N_d), and simple (N_s) contacts as a function of shape irregularity r/L ; (b) Average force carried by triple (f_t), double (f_d), and simple (f_s) contacts normalized by the mean force in the sample as a function of r/L .

Figure 5(a) displays the evolution of N_s , N_d , and N_t with r/L . We see that the nature of contacts changes dramatically: the proportion N_t of triple contacts decreases significantly with increasing r/L , while N_s becomes more prevalent. The number of double contacts N_d remain relatively constant. This shows that even small amount of shape irregularity fundamentally alters the network topology by hindering the formation of face-face contacts.

Figure 5(b) shows the average force carried by each type of contact as a function of r/L . The forces are normalized by the mean force $\langle f \rangle$. The force f_s carried by simple contacts increases slightly with increasing r/L but the forces f_d and f_t carried by the double and triple contacts, respectively, remain constant. Interestingly, the simple contacts, representing the highest proportion of contacts, carry the lowest level of force in all cases. For example, for $r/L = 0.15$, the simple contacts represent $\approx 55\%$ of contacts, but they carry an average force of $f_s = 0.65\langle f \rangle$, which is nearly half the average force carried by triple contacts ($f_t = 1.4\langle f \rangle$). This means that triple contacts tend to capture strong force chains. The double contacts carry

a force slightly above the mean force ($f_d \approx 1.1\langle f \rangle$) while they represent roughly 32% of contacts.

6 Force distributions

Figure 6 shows the probability density function (PDF) of normal contact forces f , normalized by the mean $\langle f \rangle$ for regular icosahedra and for irregular icosahedra with $r/L = 0.15$.

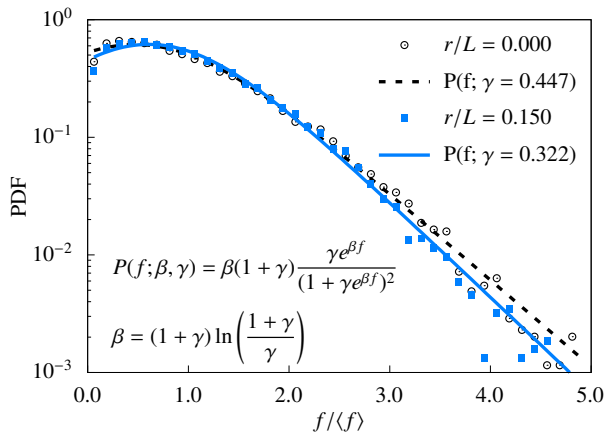


Figure 6. Probability density function of normal forces f normalized by the mean value $f/\langle f \rangle$ for $r/L = 0$ and $r/L = 0.15$. The solid lines are fits by the analytical model shown in the inset [11].

We see that the PDF is narrower in the irregular case with slightly lower number of strong forces, indicating increased homogeneity. To capture this change, we fitted the PDFs by the following form [11]:

$$P(f) = \beta(1 + \gamma) \frac{\gamma e^{\beta f}}{(1 + \gamma e^{\beta f})^2} \quad \text{with} \quad \beta = (1 + \gamma) \ln\left(\frac{1 + \gamma}{\gamma}\right)$$

The value γ varies from 0.447 for $r/L = 0$ to 0.322 for $r/L = 0.15$, in agreement with the narrowing of the distribution due to the more disordered positions of the particles as observed in the radial distribution functions in Fig. 3.

7 Conclusion

Using DEM simulations of isotropically compressed irregular icosahedra, we investigated the effect of statistical shape irregularity on granular packings. Key findings are: (1) Increased irregularity disrupts local positional order, evidenced by a broadened radial distribution function. (2) While packings remain isostatic, the contact network shifts from stabilizing triple contacts towards more numerous, weaker single contacts. (3) The force PDFs become

narrower, indicating increased homogeneity. Our results suggest that even small statistical particle-to-particle shape variations are crucial for the granular microstructure and force transmission. Future work will explore these effects in frictional systems and the effect of shape variability of the shear strength of granular materials of different particle shapes.

References

- [1] CEGEO, B. Saint-Cyr, K. Szarf, C. Voivret, E. Azéma, V. Richefeu, J.Y. Delenne, G. Combe, C. Nouguier-Lehon, P. Villard et al., Particle shape dependence in 2d granular media, *Europhysics Letters* **98**, 44008 (2012).
- [2] S. Zhao, J. Zhao, A poly-superellipsoid-based approach on particle morphology for dem modeling of granular media, *Int J Numer Anal Methods Geomech* **43**, 2147 (2019). [10.1002/nag.2951](https://doi.org/10.1002/nag.2951)
- [3] J.F. Ferrellec, G.R. McDowell, A method to model realistic particle shape and inertia in DEM, *Granular Matter* **12**, 459 (2010). [10.1007/s10035-010-0205-8](https://doi.org/10.1007/s10035-010-0205-8)
- [4] T.D. Tran, S. Nezamabadi, J.P. Bayle, L. Amarsid, F. Radjai, Effect of interlocking on the compressive strength of agglomerates composed of cohesive nonconvex particles, *Advanced Powder Technology* **36**, 104780 (2025). [10.1016/j.apt.2025.104780](https://doi.org/10.1016/j.apt.2025.104780)
- [5] M. Lu, G.R. McDowell, The importance of modelling ballast particle shape in the discrete element method, *Granular Matter* **9**, 69 (2007). [10.1007/s10035-006-0021-3](https://doi.org/10.1007/s10035-006-0021-3)
- [6] A.X. Jerves, R.Y. Kawamoto, J.E. Andrade, Effects of grain morphology on critical state: A computational analysis, *Acta Geotechnica* **11**, 493 (2016). [10.1007/s11440-015-0422-8](https://doi.org/10.1007/s11440-015-0422-8)
- [7] D.H. Nguyen, É. Azéma, F. Radjai, P. Sornay, Effect of size polydispersity versus particle shape in dense granular media, *Physical Review E* **90**, 012202 (2014).
- [8] D.H. Nguyen, É. Azéma, P. Sornay, F. Radjai, Effects of shape and size polydispersity on strength properties of granular materials, *Physical Review E* **91**, 032203 (2015). [10.1103/PhysRevE.91.032203](https://doi.org/10.1103/PhysRevE.91.032203)
- [9] V. Richefeu, G. Combe, P. Villard, J.Y. Delenne, L. Amarsid, S. Nezamabadi, F. Radjai, J.M. Vanson, R. Prat, P. Mutabaruka, Rockable (2025), <https://hal.univ-grenoble-alpes.fr/hal-04933604>
- [10] D.C. Vu, L. Amarsid, J.Y. Delenne, V. Richefeu, F. Radjai, Macro-elasticity of granular materials composed of polyhedral particles, *Granular Matter* **26**, 6 (2024). [10.1007/s10035-023-01382-3](https://doi.org/10.1007/s10035-023-01382-3)
- [11] F. Radjai, Modeling force transmission in granular materials, *Comptes Rendus. Physique* **16**, 3 (2015). [10.1016/j.crhy.2015.01.003](https://doi.org/10.1016/j.crhy.2015.01.003)